

A NOVEL FAULT DIAGNOSIS METHOD FOR MARINE BLOWER WITH VIBRATION SIGNALS

Guohua Yan*

Yihuai Hu

Jiawei Jiang

Shanghai Maritime University, Shanghai, China

* Corresponding author: yanguoahuabetter@163.com (G. Yan)

ABSTRACT

The vibration signals on marine blowers are non-linear and non-stationary. In addition, the equipment in marine engine room is numerous and affects each other, which makes it difficult to extract fault features of vibration signals in the time domain. This paper proposes a fault diagnosis method based on the combination of Ensemble Empirical Mode Decomposition (EEMD), an Autoregressive model (AR model) and the correlation coefficient method. Firstly, a series of Intrinsic Mode Function (IMF) components were obtained after the vibration signal was decomposed by EEMD. Secondly, effective IMF components were selected by the correlation coefficient method. AR models were established and the power spectrum was analysed. It was verified that blower failure can be accurately diagnosed. In addition, an intelligent diagnosis method was proposed based on the combination of EEMD energy and a Back Propagation Neural Network (BPNN), with a correlation coefficient method to get effective IMF components, and the energy components were calculated, normalised as a feature vector. Finally, the feature vector was sent to the BPNN for training and state recognition. The results indicated that the EEMD-BPNN intelligent fault diagnosis method is suitable for highly accurate fault diagnosis of marine blowers.

Keywords: Fault diagnosis, Marine blower, EEMD, Correlation coefficient, AR spectrum, BPNN

INTRODUCTION

As an important equipment in the marine engine room, the blower is responsible for transporting air required by the entire ship and ensuring the normal operation of the ship. Inadequate machinery maintenance will increase equipment failure, posing a threat to the ocean environment, affecting performance, having a great impact in terms of business losses by reducing ship availability, increasing downtime and moreover increasing the potential for major accidents occurring and endangering lives on board [1]. In the past, this work was accomplished through condition-based and time-based maintenance, which depends heavily on human cognition and experience [2,3]. It is difficult to meet the

development needs of large-scale, intelligent and unmanned ships. Especially, subsystems in marine machinery are coupled with each other, and a minor fault may bring a chain effect to related subsystems, thus amplifying the damage caused by the fault [4]. Consequently, it is necessary to diagnose blower faults and carry out condition-based maintenance. The maintenance measures have important practical significance – they ensure the safe operation of mechanical equipment and reduce the rate of occurrence of significant accidents [5].

The traditional fault diagnosis method includes over-current detection and over-voltage detection. There are also new methods including Short-time Fourier Transform (STFT) [7], Wavelet Transform (WT) [8], Empirical Mode Decomposition (EMD) [9], and Artificial Neural Networks

(ANN) [10]. The classical Fast Fourier Transform (FFT) can only reflect the overall characteristics of a vibration signal. The short-time Fourier transform obtains the relationship between time and frequency by adding a narrow window function, but it still cannot meet the requirements of high frequency resolution in the low-frequency region and high time resolution in the high-frequency region. Non-intrusive vibration measurement is used for effective identification of journal bearing operation in rotating machinery [11,12], but the vibration signal is a nonlinear and non-stationary signal, which is not suitable for analysis with the Fourier transform. Although WT and EMD are effective in processing nonlinear and non-stationary signals, they also have some problems. For example, in the wavelet transform method, the suitable wavelet bases should be pre-set, meaning that it lacks self-adaptability. On the other hand, empirical mode decomposition is a type of adaptive time–frequency analysis algorithm [13]; Ensemble Empirical Mode Decomposition (EEMD) [14] can overcome the modal aliasing effect of EMD effectively [15]. However, EEMD still has two issues that need to be addressed. First is how to pick out the IMF(s) which contains sufficient fault feature information. Second, in the case of strong background noise and for early failure, EEMD is not ideal to extract the fault feature [15]. The AR model is the most basic and most widely used mathematical model in time series analysis. It condenses the characteristics and working status of the system. It can not only diagnose faults, but also predict potential faults early. Table 1 shows the advantages and disadvantages of several typical fault feature extraction methods for fault diagnosis.

Schoen et al. used Fast Fourier Transform (FFT) to extract the most pertinent information for motor fault diagnosis, and the results show that they can accurately extract fault features [19]. Wang et al. proposed a novel intelligent fault-diagnosis method based on generalised composite multiscale weighted permutation entropy (GCMWPE), and this method was able to correctly diagnose bearing faults [13]. Khelil et al. used ANN to monitor engine health and diagnose faults. Experiments indicated that the fault can be detected instantaneously at its early stage [20]. Jia et al. combined integrated EEMD and grey theory to remove noise in the vibration signal, and the denoising effect was better than wavelet denoising and other methods, but the time required was longer, which limits its application [21].

Several classifiers have been used in the fault diagnosis of marine equipment, such as expert systems [22], Artificial Neural Networks [10], and Support Vector Machines (SVM) [23]. Although SVM can handle small samples and nonlinear and non-stationary data very well, the SVM classifier performance is greatly affected by selecting the penalty parameter (c) and kernel parameter (g). Incorrect selection will directly affect the diagnosis accuracy and its generalisation ability [11]. In recent years, BPNN has been comprehensively exploited in intelligent fault diagnosis because of its predominant self-adaptation and input–output nonlinear mapping [24]. It is necessary to find a novel intelligent method for fault diagnosis in marine blowers.

Tab. 1. Comparative classic studies of fault feature extraction methods

Method	Advantages	Disadvantages
FFT	It can reflect the overall characteristics of the signal (time domain or frequency domain)	1. Not suitable for non-stationary and non-linear signals 2. Inability to reflect the relationship between time and frequency
STFT	No cross-terms interference and overlaps [16]	Poor time–frequency resolution [17]
WT	1. Time-frequency windows with different sizes at different times and frequencies 2. Suitable for non-stationary and non-linear signals	Limited by Heisenberg’s uncertainty principle
EMD [18]	1. The signal analysis turns out to be adaptive 2. Suitable for non-stationary and non-linear signals	1. Mode mixing problem 2. Boundary effect 3. Lacks support of mathematical theory
EEMD	It can effectively suppress mode mixing	1. It is difficult to pick out effective IMF(s) 2. In the case of strong background noise and early failure, EEMD is not ideal to extract the fault feature [15]

RELATED FAULT DIAGNOSIS METHODS

EEMD

EEMD mainly reduces modal aliasing by adding several sets of white noise to the signal $x(t)$. The EEMD process is briefly explained below:

- 1) Add different white noise sequences $n_j(t)$ ($j=1,2,3,\dots,M$) to the signal $x(t)$.

$$x_j(t) = x(t) + n_j(t) \quad (1)$$

where $x_j(t)$ represents the signal after adding white noise for the j -th time; j represents the number of times white noise is added.

- 2) EMD decomposition is performed for each group $x_j(t)$, and I intrinsic mode function (IMF) components are obtained for each group, which are recorded as $C_{i,j}(t)$ ($i=1,2,3,\dots,I$; $j=1,2,3,\dots,M$), where $C_{i,j}(t)$ represents the i -th IMF obtained by EMD decomposition after adding white noise amplitude for the j -th time.
- 3) If $j < M$, let $j=j+1$ and repeat process 2;
- 4) The above IMFs are calculated by the overall average, and the final IMF is

$$C_i(t) = \frac{1}{M} \sum_{j=1}^M C_{i,j}(t) \quad (2)$$

where $C_i(t)$ represents the i IMFs obtained by EEMD, and M represents the number of averages.

- 5) The original signal is

$$x(t) = C_i(t) + \text{Res} \quad (3)$$

where Res is the residual component of EEMD.

AR MODEL
The power spectrum estimation based on AR model parameter modelling can effectively improve the frequency resolution. Due to its extension, it can effectively analyse short-sample signals, overcome the windowing effect of Hilbert's separation algorithm, and the resulting spectrum is smoother and different. The spectrum in this case is easier to distinguish. The basic idea of AR spectrum estimation is: first to establish an AR model for the time-series signal, and then to use the model coefficients to calculate the signal's self-power spectrum. The general expression of the AR(N) model is

$$y(n) = B(n) - \sum_{k=1}^n a_k y(n-k) \quad (4)$$

where $y(n)$ is the autoregressive time series; $B(n)$ is the finite bandwidth white noise with a normal distribution with zero mean and variance σ^2 ; N is the order of the model.

CORRELATION COEFFICIENT METHOD

EEMD can decompose a time-domain signal into a series of IMF components and a residual component from high to low frequencies [25]. The actual collected vibration signal contains some noise, the existence of which affects the accuracy of signal analysis. Using only EEMD to decompose the signal cannot remove the noise. Singh et al. calculated the correlation coefficient between each IMF and the original signal, and selected the most correlated IMF components for recombination, so as to achieve the purpose of removing the noise in the signal [26]. The calculation formula of the correlation coefficient between signal A and B is as follows:

$$P(t) = \frac{\text{COV}(A,B)}{\sqrt{D(A)}\sqrt{D(B)}} \quad (5)$$

where $P(t)$ is the correlation coefficient, $\text{COV}(A,B)$ is the covariance of signal A and signal B, and $\sqrt{D(A)}$ and $\sqrt{D(B)}$ are the variance.

The larger the $P(t)$, the higher the correlation between A and B. According to the value of the correlation coefficient, the interference component in the signal can be removed.

ENERGY PRINCIPLE

After a fault of the marine blower occurs, the energy contained in its vibration signal will also change. According to the different energy distribution under different working conditions, the fault type can be identified [27]. After the vibration signals under different working conditions are decomposed by EEMD, the energy of each IMF is different, which can be used as a fault feature.

EXPERIMENT AND ANALYSIS

EXPERIMENTAL SETUP

A test bench is used to simulate some typical blower faults in the laboratory. The experimental system is mainly composed of the blower test bench, vibration sensor, photoelectric speed tester, National Instruments(NI) data acquisition module and computer.

Three kinds of motor faults were simulated: an inter-rotor short circuit (the U-phase short circuit ratio is 18.6%), a rotor bar breaking fault and a bearing abrasion fault; There were four kinds of faults: unbalanced blades, blocked air outlets, loose motor bolts, and combined faults with loose bolts and unbalanced blades, as shown in Fig. 1. The short circuit is the most serious failure of the blower, whereas bearing wear is not serious, but will increase the power loss [28]. The vibration sensor was installed above the end cover of the motor output bearing as shown in Fig. 2. The rotating speed of the blower was measured by a hand-held speed detector irradiating the reflective strip pasted on the blower, as shown in Fig. 1. The sampling frequency was 2048 Hz and the sampling time length was 2s. The main parameters of the blower are shown in Table 2.



Fig. 1. Blower imbalance fault setting



Fig. 2. Blower test bench

Tab. 2. The main parameters of the blower

Rated power	1.1 kW	Rated speed	1430 r/min
Capacity	1500~2200 m ³ /h	Power factor	0.89
Motor type	Three-phase cage asynchronous motor	Rated current	4.6 A

EXPERIMENTAL RESULTS

EEMD is used to decompose the vibration signals. The standard deviation of auxiliary white noise is 0.3 times that of the original signal, and the number of white noise integration m is 100. Taking the normal condition vibration signal of the motor as an example, 16 IMF components and one residual component are obtained after EEMD decomposition, as shown in Fig. 3.

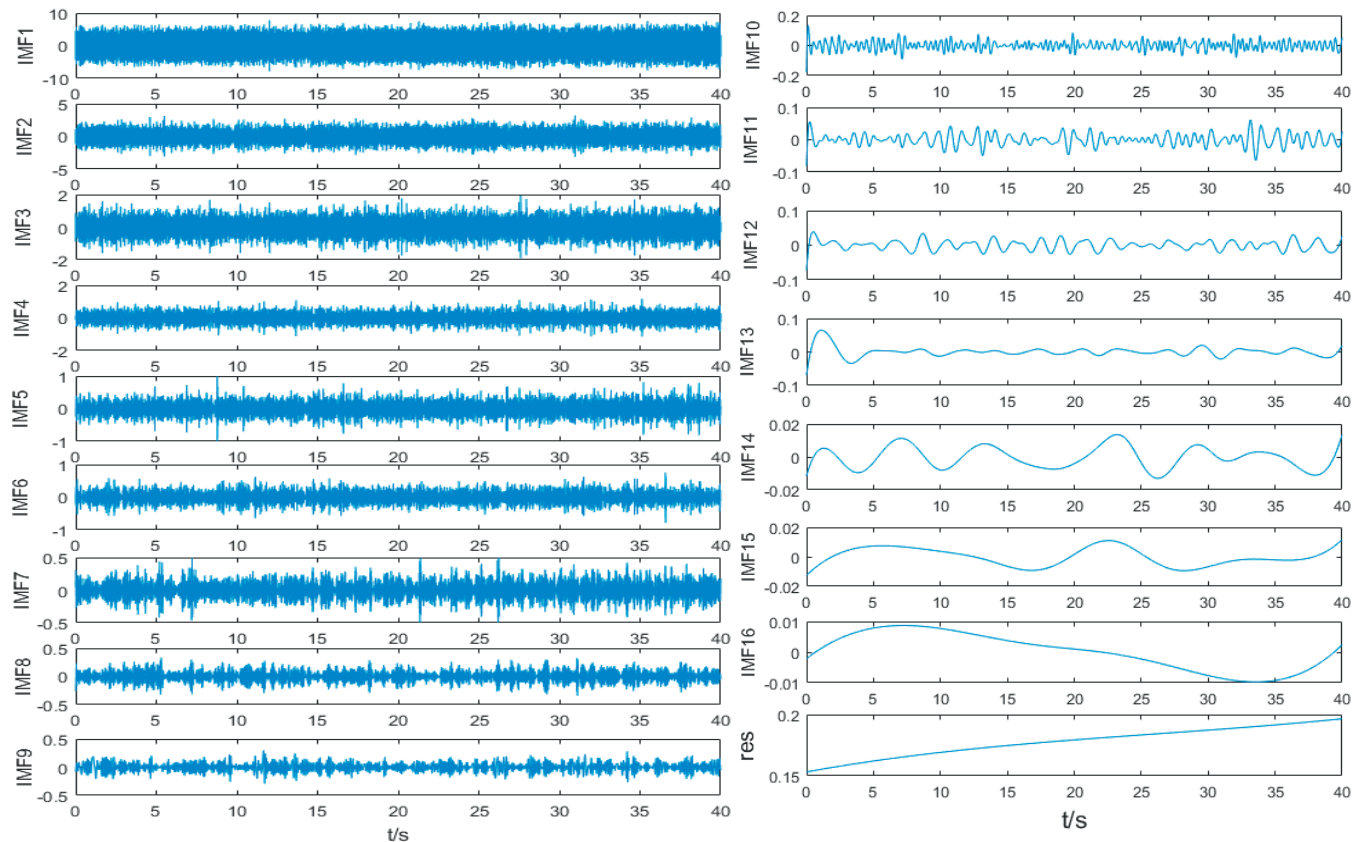


Fig. 3. EEMD decomposition of motor vibration signal under normal condition

As described above, the correlation coefficients between all IMFs and the original signal are calculated, and the results are shown in Table 3.

Tab. 3. Correlation coefficients of each IMF and the original signal under normal conditions

IMF1	IMF2	IMF3	IMF4	IMF5	IMF6	IMF7	IMF8
0.5838	0.2929	0.7493	0.5013	0.0973	0.0692	0.5013	0.0974
IMF9	IMF10	IMF11	IMF12	IMF13	IMF14	IMF15	IMF16
0.0838	0.1003	0.0383	0.0117	0.0025	0.0010	0.0004	0.0005

It can be seen from Table 3 that IMF1~IMF4 and IMF7 have relatively large correlation coefficients with the original signal, which can be considered as the effective component of the signal. These five IMFs components are selected for reconstruction to achieve signal noise reduction.

FFT ANALYSIS

After the noise reduction of the vibration signals, the traditional FFT analysis method is used to analyse them, taking the normal condition and short-circuit fault of the motor as an example. When the motor has a short-circuited fault, the grid frequency is 50 Hz, the measured speed is 1458 r/min, and the slip rate s is 0.028. The FFT analysis results under normal and short-circuit faults are shown in Fig. 4.

FAULT DIAGNOSIS

MOTOR FAULT DIAGNOSIS BASED ON EEMD-AR SPECTRUM

The AR model is mainly used for stationary processes, while EEMD decomposes complex nonlinear non-stationary signals into a number of single-component signals with zero

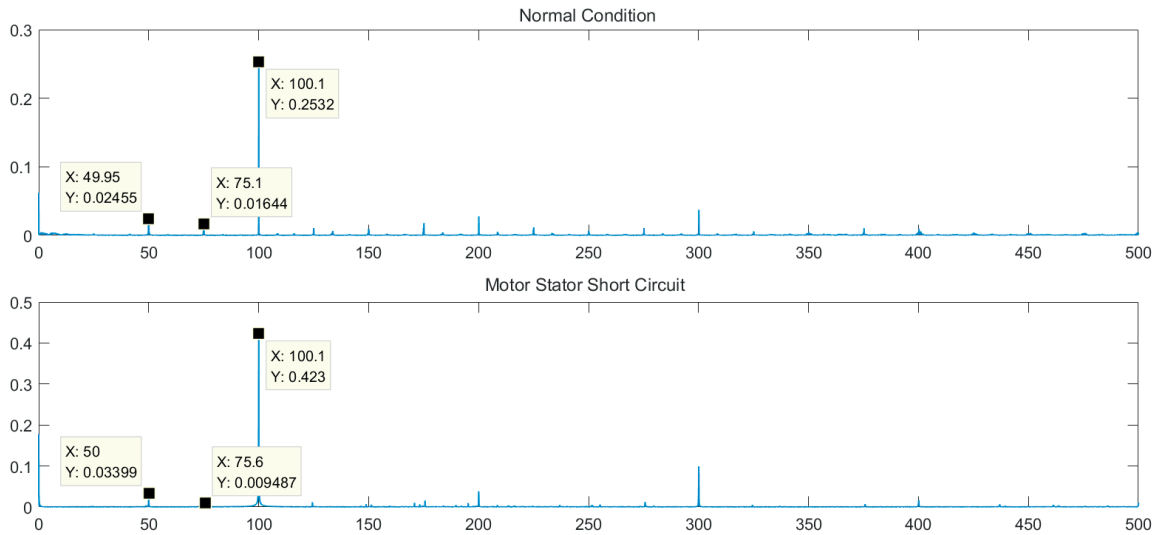


Fig. 4. FFT Analysis of motor in normal condition and stator short circuit

As can be seen from the spectrum diagram in Fig. 4, the amplitude of the spectrum with a motor short-circuit fault at 50 Hz is larger than that with the normal condition, but there is almost no difference at 75 Hz, where it is difficult to distinguish. In both cases, the amplitude reaches the maximum at 100 Hz, and the amplitude of the motor short-circuit fault is much larger than the normal condition. The motor is a 4-pole asynchronous motor, so the amplitude reaches the maximum at four times the rotation frequency. Due to the stator short-circuit fault of the motor, the short-circuit phase current increases, which destroys the magnetic field balance and causes imbalance of the electromagnetic force. The final amplitude is larger than the normal condition at twice and four times the frequency, and the fault characteristics are obvious. Therefore, the motor short-circuit fault can be diagnosed by FFT. By analysing other blower faults, the results show that this method can also distinguish them effectively.

mean and which are locally symmetrical with respect to the time axis, which is equivalent to linearising and smoothing the original signal. Therefore, a diagnostic method combining EEMD and the AR spectrum is proposed, which can combine the advantages of both. That is, the signal is first decomposed by EEMD, and then the correlation between each IMF component and the original signal is calculated, and the IMF with the largest correlation coefficient is selected to establish the AR model.

$$c_i(t) + \sum_{k=1}^m \varphi_{ik} c_i(t-k) = e_i(t) \quad (5)$$

where $c_i(t)$ is the IMF component that satisfies the condition; φ_{ik} is the model parameter of the AR model; $e_i(t)$ is the residual of the AR model; m is the model order of the AR model. The diagnosis process based on the EEMD spectrum is shown in Fig. 5.

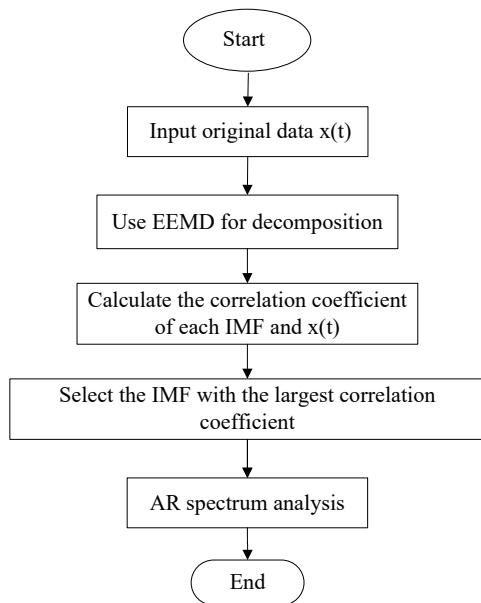


Fig. 5. Diagnosis process based on EEMD spectrum

The four working conditions of the motor are analysed according to this method. For each work situation, we select the 4 largest correlation coefficients to establish an AR model, then calculate the power spectrum. The EEMD-AR spectrum obtained is shown in Fig. 6.

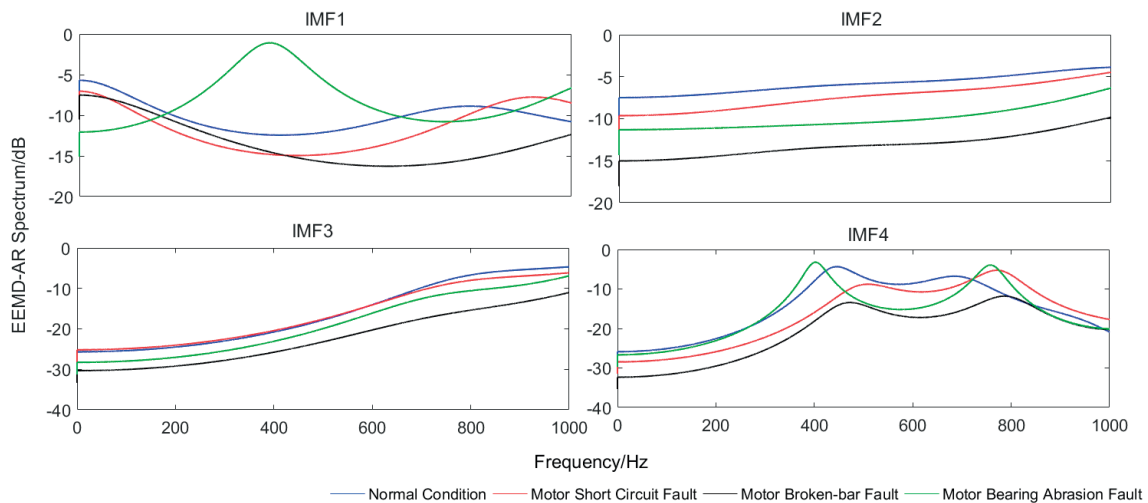


Fig. 6. EEMD-AR spectrum in four conditions

It can be seen from the AR spectrum of the IMF1 component in Fig. 6 that in the frequency band of 0-550 Hz, the energy of the motor in the normal condition, with a short-circuit fault and a broken bar fault decreases slowly and has little difference, while the amplitude of the bearing wear fault first increases and then decreases, and reaches the maximum value at the frequency of 400 Hz. The motor bearing wear fault can be clearly identified in this frequency band. In other frequency bands it is difficult to distinguish between the four conditions. In the AR spectrum of the IMF2 component, the

energy of the four conditions increases slowly in the analysed frequency band without intersection. Therefore, the four states can be accurately judged by analysing the energy of the IMF2 component. In the AR spectrum of the IMF3 component, the energy of the normal state and short-circuit fault are almost the same in the whole analysed frequency band, which makes it difficult to judge the two states. Although the energy of the motor bearing wear and broken bar fault increases slowly in this frequency band and has no intersection, the energy is similar and the diagnosis effect is not ideal. In the AR spectrum of the IMF4 component, in the frequency band of 0-300 Hz, the energy of the short-circuit fault and broken bar fault increases slowly but gets closer and closer, but the two states can still be distinguished. The energy of the other two states is too close to distinguish. Other frequency bands have serious waveform overlap, so it is impossible to distinguish the working conditions of the motor.

Based on the analysis above, the AR spectrum of the IMF1 ~ IMF4 components can be used to identify four motor conditions, among which the AR spectrum of the IMF1 component has the best effect on identifying bearing wear fault, but only this fault can be identified; the IMF2 component can identify four states, and the effect is the best; the AR spectrum of the IMF3 component makes it difficult to identify the fault; the AR spectrum of the IMF4 component can only identify two faults in the inherent frequency band, which is limited in diagnosis.

FAULT DIAGNOSIS BASED ON BPNN

Back Propagation Neural Network

BPNN has been comprehensively exploited in intelligent fault diagnosis because of its predominant self-adaptation and input-output nonlinear mapping. BPNN usually consists of an input layer, several hidden layers and an output layer [29].

The sample enters from the input layer and passes through the network structure layer by layer to the output layer. If the output value and the expected value are within the error range, it ends. Otherwise, the error between the actual value and the expected value is adjusted layer by layer in reverse and

each layer's weight is repeatedly modified until convergence [30]. The basic structure of the BPNN is shown in Fig. 7.

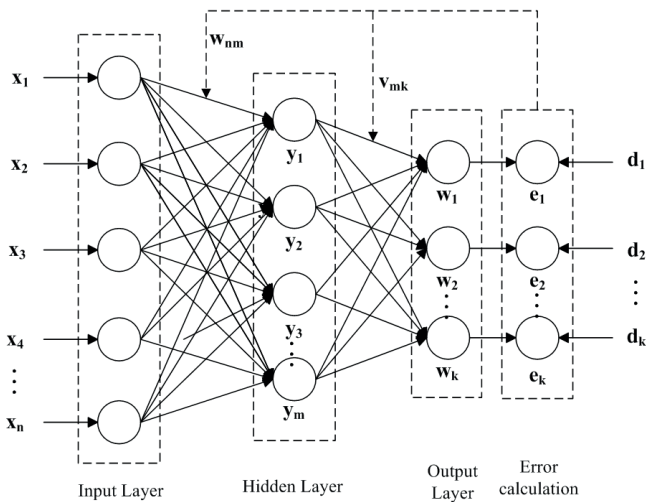


Fig. 7. The basic structure of the BPNN

Fault feature extraction

The IMF component contains the current operating status information of the blower, and the energy of the four IMF components with correlation coefficients ranging from large to small and greater than 0.2 is selected as the fault feature, and then normalised to constitute a 4-dimensional feature matrix as the input of the BPNN. The energy calculation steps are as follows:

Step 1: Select effective IMFs components by the correlation coefficient method

Step 2: Calculate the energy of each IMF selected

$$E_i = \sum C_{ik}^2(t) \quad (7)$$

where C_{ik} is the amplitude of discrete points of each IMF component.

Fault diagnosis expected output

The blower has eight different working conditions, so the output is 8 nodes. The expected values of the different fault output nodes are shown in Table 4.

Tab. 4. BPNN expected output

State	Expected output
Normal	0000 0001
Broken rotor bar	0000 0010
Stator short circuit	0000 0100
Bearing abrasion	0000 1000
Unbalanced blades	0001 0000
Blocked air outlets	0010 0000
Loose motor base bolts	0100 0000
Coupling faults	1000 0000

BPNN main parameters

The learning rate, the number of hidden layers and the number of hidden layer nodes determine the performance of the BPNN, but these parameters can only be determined by experience or empirical formulae. A large number of experiments and formula calculations show that the correct rate is the highest when the hidden layer structure is 4 layers [31]. The main parameters of the BPNN are shown in Table 5.

Tab. 5. The main parameters of the BPNN

Number of nodes in the input layer	4
Number of nodes in the output layer	8
Number of hidden layer	4
Number of hidden layer nodes	8,16,32,8
Learning rate	0.05
Training function	trainlm
Training goals	0.00001
Maximum number of iterations	300

BPNN diagnostic results

We collect 160 groups of data of vibration signals of the blower under normal conditions and motor short-circuit, broken bar and bearing wear faults; and 120 groups of blade imbalance, loose motor base, blower air outlet blockage and looseness plus unbalanced coupling fault. Each group has a sampling time of 2 seconds, and a total of 1120 groups of data are collected. 70% of them are used for training the BPNN and 30% for testing. The training results are shown in Fig. 8, and it can be seen that when the iteration reaches 113 times, the value of training error meets the accuracy requirement. The diagnostic accuracy of the BPNN is shown in Table 6 where it is seen that the comprehensive and accurate recognition rate of the test samples using the BPNN reached 96.5%. Therefore, the combination of the EEMD energy and the correlation coefficient method can effectively extract the characteristic information of the marine blower, and reliably realise fault identification through the BPNN.

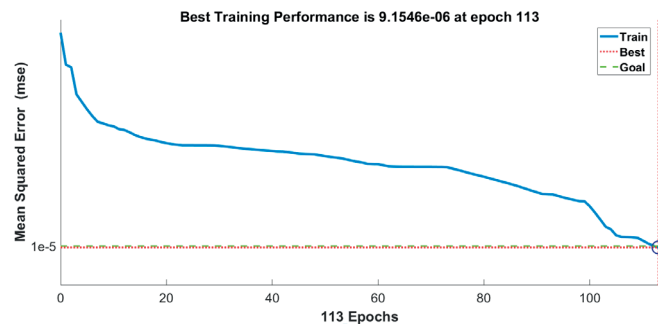


Fig. 8. Training results of the EEMD-BPNN

Tab. 6. Diagnostic accuracy of the BPNN

Type	Number of training samples	Number of test samples	Number of misjudgments	Correct rate
Normal	110	50	0	100%
Stator short circuit	110	50	4	92%
Broken rotor bar	110	50	2	96%
Bearing abrasion	110	50	1	98%
Unbalanced blades	84	36	0	100%
Blocked air outlets	84	36	3	88.9%
Loose motor base bolts	84	36	1	97.2%
Coupling faults	84	36	0	100%
Total	776	344	12	96.5%

CONCLUSIONS

Aiming at the non-linear and non-stationary characteristics of the vibration signal of a marine blower, and the problem of large engine room vibration and noise interference, this research proposes a fault diagnosis method based on EEMD, the AR model and the correlation coefficient method. This method can not only extract the effective components in the signal, but also combine the advantages of the EEMD and AR models. Through the analysis of the experimental data of the blower test bench, the method can accurately identify faults.

The energy contained in the vibration signal of the blower under different working conditions is different. This research proposes a fault feature extraction method of the marine blower based on the EEMD energy and correlation coefficient method. The effective components of the vibration signal are selected by the correlation coefficient method, and the energy of the IMF components of different frequency bands is used to construct the feature vector and as input into the established BPNN fault recognition model after normalisation. Verified by a large number of test samples, the fault identification results show that the EEMD-BPNN method can effectively extract the fault characteristic information of the marine blower, and accurately identify the fault type.

Future work will aim to optimise the BPNN to reduce the impact of inherent defects of its own structure, for example, by using an adaptive learning rate method to reduce the BPNN training time and increase its accuracy. Finally, an intelligent fault diagnosis system with higher accuracy for marine blowers is designed.

ACKNOWLEDGMENTS

This work was supported by the Science & Technology Commission of Shanghai Municipality and Shanghai Engineering Research Center of Ship Intelligent Maintenance and Energy Efficiency under Grant 20DZ2252300

DECLARATION OF COMPETING INTEREST

The authors declare that they have no known competing financial interests or personal relationships that could have appeared to influence the work reported in this paper.

REFERENCES

1. I. Lazakis, Y. Raptodimos, T. Varelas, "Predicting ship machinery system condition through analytical reliability tools and artificial neural networks," *Ocean Engineering*, vol. 152, pp. 404-415, 2018.
2. I. Lazakis, C. Gkerekos, and G. Theotokatos, "Investigating an SVM-driven, one-class approach to estimating ship systems condition," *Ships and Offshore Structures*, vol. 14, no. 5, pp. 432-441, 2019, doi: 10.1080/17445302.2018.1500189.
3. Y. Raptodimos and I. Lazakis, "Using artificial neural network-self-organising map for data clustering of marine engine condition monitoring applications," *Ships and Offshore Structures*, vol. 13, no. 6, pp. 649-656, 2018, doi: 10.1080/17445302.2018.1443694.
4. Y. Tan, J. Zhang, H. Tian, D. Jiang, L. Guo, G. Wang, and Y. Lin, "Multi-label classification for simultaneous fault diagnosis of marine machinery: A comparative study," *Ocean Engineering*, vol. 239, p. 109723, 2021, ISSN 0029-8018, <https://doi.org/10.1016/j.oceaneng.2021.109723>.
5. H. Habibi, I. Howard, and S. Simani, "Reliability improvement of wind turbine power generation using model-based fault detection and fault tolerant control: A review," *Renewable Energy*, vol. 135, pp. 877-896, 2019, ISSN 0960-1481, <https://doi.org/10.1016/j.renene.2018.12.066>.
6. K. Satpathi, A. Ukil, and J. Pou, "Short-Circuit Fault Management in DC Electric Ship Propulsion System: Protection Requirements, Review of Existing Technologies and Future Research Trends," *IEEE Transactions on Transportation Electrification*, vol. 4, no. 1, pp. 272-291, March 2018, doi: 10.1109/TTE.2017.2788199.
7. É. M. Lima, C. M. dos Santos, N. S. D. Brito, B. A. de Souza, R. de Almeida Coelho, and H. Gayoso Meira Suassuna de Medeiros, "High impedance fault detection method based on the short-time Fourier transform," *IET Gener. Transm. Distrib.*, vol. 12, pp. 2577-2584, 2018, <https://doi.org/10.1049/iet-gtd.2018.0093>.
8. K. M. Silva, B. A. Souza, and N. S. D. Brito, "Fault detection and classification in transmission lines based on wavelet transform and ANN," *IEEE Transactions on Power Delivery*, vol. 21, no. 4, pp. 2058-2063, Oct. 2006, doi: 10.1109/TPWRD.2006.876659.

9. Y. Cheng, Z. Wang, B. Chen, W. Zhang, and G. Huang, "An improved complementary ensemble empirical mode decomposition with adaptive noise and its application to rolling element bearing fault diagnosis," *ISA Transactions*, vol. 91, pp. 218-234, 2019, ISSN 0019-0578, <https://doi.org/10.1016/j.isatra.2019.01.038>.
10. M. E. Baran and N. R. Mahajan, "Overcurrent Protection on Voltage-Source-Converter-Based Multiterminal DC Distribution Systems," *IEEE Transactions on Power Delivery*, vol. 22, no. 1, pp. 406-412, Jan. 2007, doi: 10.1109/TPWRD.2006.877086.
11. M. Moschopoulos, G. N. Rossopoulos, and C. I. Papadopoulos, "Journal Bearing Performance Prediction Using Machine Learning and Octave-Band Signal Analysis of Sound and Vibration Measurements," *Polish Marit. Res.*, vol. 28, no. 3, 2021, doi: 10.2478/pomr-2021-0041.
12. N. Vulić, K. Bratić, B. Lalić, and L. Stazić, "Implementing Simulationx in the Modelling of Marine Shafting Steady State Torsional Vibrations," *Polish Marit. Res.*, vol. 28, no. 2, 2021, doi: 10.2478/pomr-2021-0022.
13. Z. Wang, L. Yao, G. Chen, and J. Ding, "Modified multiscale weighted permutation entropy and optimized support vector machine method for rolling bearing fault diagnosis with complex signals," *ISA Transactions*, vol. 114, pp. 470-484, 2021, ISSN 0019-0578, <https://doi.org/10.1016/j.isatra.2020.12.054>.
14. F. Wang, "Pulsation Signals Analysis of Turbocharger Turbine Blades based on Optimal EEMD and TEO," *Polish Marit. Res.*, vol. 26, no. 3, 2019, doi: 10.2478/pomr-2019-0048.
15. H. Li, T. Liu, X. Wu, and S. Li, "Research on test bench bearing fault diagnosis of improved EEMD based on improved adaptive resonance technology," *Measurement*, vol. 185, p. 109986, 2021, ISSN 0263-2241, <https://doi.org/10.1016/j.measurement.2021.109986>.
16. S. M. Debbal and F. Berekci-Reguig, "Time-frequency analysis of the first and the second heartbeat sounds," *Applied Mathematics and Computation*, vol. 184, issue 2, pp. 1041-1052, 2007, ISSN 0096-3003, <https://doi.org/10.1016/j.amc.2006.07.005>.
17. T. Sang, "The Self-Duality of Discrete Short-Time Fourier Transform and Its Applications," *IEEE Transactions on Signal Processing*, vol. 58, no. 2, pp. 604-612, Feb. 2010, doi: 10.1109/TSP.2009.2032038.
18. J. Zheng and H. Pan, "Mean-optimized mode decomposition: An improved EMD approach for non-stationary signal processing," *ISA Transactions*, vol. 106, pp. 392-401, 2020, ISSN 0019-0578, <https://doi.org/10.1016/j.isatra.2020.06.011>.
19. R. R. Schoen, B. K. Lin, T. G. Habetler, J. H. Schlag, and S. Farag, "An unsupervised, on-line system for induction motor fault detection using stator current monitoring," *IEEE Transactions on Industry Applications*, vol. 31, no. 6, pp. 1280-1286, Nov.-Dec. 1995, doi: 10.1109/28.475698.
20. Y. Khelil, G. Graton, M. Djeziri, M. Ouladsine, and R. Outbib, "Fault Detection and Isolation in Marine Diesel Engines: A Generic Methodology," *IFAC Proceedings*, vol. 45, issue 20, pp. 964-969, 2012, ISSN 1474-6670, ISBN 9783902823090, <https://doi.org/10.3182/20120829-3-MX-2028.00164>.
21. Y. Jia, G. Li, X. Dong, and K. He, "A novel denoising method for vibration signal of hob spindle based on EEMD and grey theory," *Measurement*, vol. 169, p. 108490, 2021, ISSN 0263-2241, <https://doi.org/10.1016/j.measurement.2020.108490>.
22. T. Berredjem and M. Benidir, "Bearing faults diagnosis using fuzzy expert system relying on an Improved Range Overlaps and Similarity method," *Expert Systems with Applications*, vol. 108, pp. 134-142, 2018, ISSN 0957-4174, <https://doi.org/10.1016/j.eswa.2018.04.025>.
23. H. Wang, M. Peng, J. Wesley Hines, G. Zheng, Y. Liu, and B. R. Upadhyaya, "A hybrid fault diagnosis methodology with support vector machine and improved particle swarm optimization for nuclear power plants," *ISA Transactions*, vol. 95, pp. 358-371, 2019, ISSN 0019-0578, <https://doi.org/10.1016/j.isatra.2019.05.016>.
24. H. Qin, R. Yang, C. Guo, and W. Wang, "Fault diagnosis of electric rudder system using PSOFOA-BP neural network," *Measurement*, vol. 186, p. 110058, 2021, ISSN 0263-2241, <https://doi.org/10.1016/j.measurement.2021.110058>.
25. M. S. Hoseinzadeh, S. E. Khadem, and M. S. Sadooghi, "Quantitative diagnosis for bearing faults by improving ensemble empirical mode decomposition," *ISA Transactions*, vol. 83, pp. 261-275, 2018, ISSN 0019-0578, <https://doi.org/10.1016/j.isatra.2018.09.008>.
26. G. Singh, G. Kaur, and V. Kumar, "ECG denoising using adaptive selection of IMFs through EMD and EEMD," 2014 International Conference on Data Science & Engineering (ICDSE), 2014, pp. 228-231, doi: 10.1109/ICDSE.2014.6974643.
27. Z. Wang, R. Razzaghi, M. Paolone, F. Rachidi, "Time reversal applied to fault location in power networks: Pilot test results and analyses," *International Journal of Electrical Power & Energy Systems*, vol. 114, p. 105382, 2020, ISSN 0142-0615, <https://doi.org/10.1016/j.ijepes.2019.105382>.

28. P. Bzura, "Diagnostic Model of Crankshaft Seals," Polish Marit. Res., vol. 26, no. 3, 2019, doi: 10.2478/pomr-2019-0044.
29. Z. Ye and M. K. Kim, "Predicting electricity consumption in a building using an optimized back-propagation and Levenberg–Marquardt back-propagation neural network: Case study of a shopping mall in China," Sustainable Cities and Society, vol. 42, pp. 176-183, 2018, ISSN 2210-6707, <https://doi.org/10.1016/j.scs.2018.05.050>.
30. H. K. Aggarwal, M. P. Mani, and M. Jacob, "MoDL: Model-Based Deep Learning Architecture for Inverse Problems," IEEE Transactions on Medical Imaging, vol. 38, no. 2, pp. 394-405, Feb. 2019, doi: 10.1109/TMI.2018.2865356.
31. Z. Yang, C. Kong, Y. Wang, X. Rong, and L. Wei, "Fault diagnosis of mine asynchronous motor based on MEEMD energy entropy and ANN," Computers & Electrical Engineering, vol. 92, p. 107070, 2021, ISSN 0045-7906, <https://doi.org/10.1016/j.compeleceng.2021.107070>.

CONTACT WITH THE AUTHORS

Guohua Yan

e-mail: yanguohuabetter@163.com

Shanghai Maritime University,
No.1550, Harbour Avenue, Pudong New Area,
Shanghai, 201306 Shanghai,
CHINA

Yihuai Hu

e-mail: yhhu@shmtu.edu.cn

Shanghai Maritime University,
No.1550, Harbour Avenue, Pudong New Area,
Shanghai, 201306 Shanghai,
CHINA

Jiawei Jiang

e-mail: oliver1992@vip.qq.com

Shanghai Maritime University,
No.1550, Harbour Avenue, Pudong New Area,
Shanghai, 201306 Shanghai,
CHINA